

Cross Section Measurements of Neutron Induced Reactions on GaAs using Monoenergetic Beams from 7.5 to 15 MeV

R Raut^{1,4}, A S Crowell^{1,4}, B Fallin^{1,4}, C R Howell^{1,4}, C Huibregtse^{1,4},
J H Kelley^{2,4}, T Kawano³, E Kwan^{1,4}, G Rusev^{1,4},
A P Tonchev^{1,4}, W Tornow^{1,4}, D J Vieira³, J B Wilhelmy³

¹ Duke University, Durham, North Carolina 27708-0308, USA

² North Carolina State University, Raleigh, North Carolina 27695-8202, USA

³ Los Alamos National Laboratory, Los Alamos, New Mexico 87545, USA

⁴ Triangle Universities Nuclear Laboratory, Durham, North Carolina 27708-0308, USA

E-mail: raut@tunl.duke.edu

Abstract.

Cross section measurements for the neutron induced reactions on GaAs have been carried out at ten different neutron energies from 7.5 to 15 MeV, using the activation technique. The monoenergetic neutron beams were produced via the $^2\text{H}(\text{d},\text{n})^3\text{He}$ reaction, known for its high neutron yield in the chosen energy regime. GaAs samples were activated along with the Au and Al monitor foils, for estimating the incident neutron flux. The induced activity was measured using high resolution γ -ray spectroscopy. Five reaction channels viz., $^{69}\text{Ga}(n, 2n)^{68}\text{Ga}$, $^{69}\text{Ga}(n, p)^{69\text{m}}\text{Zn}$, $^{71}\text{Ga}(n, p)^{71\text{m}}\text{Zn}$, $^{75}\text{As}(n, 2n)^{74}\text{As}$ and $^{75}\text{As}(n, p)^{75}\text{Ge}$, have been reported for the comprehensive cross section measurements. The results are compared with the existing literature data and the available evaluations. Statistical model calculations, based on the Hauser-Feshbach formalism, have been carried out using the TALYS and EMPIRE codes and are compared with the experimental values.

1. Introduction

GaAs is an important semiconductor with vast vistas of application in research and industry. It is often preferred over other semiconductors in the construction of microwave frequency integrated circuits, infrared light emitting diodes, laser diodes, solar cells and optical windows. Exposure of GaAs to a flux of fast neutrons is expected to initiate transmutation processes within the semiconductor, leading to an increase in the impurity content and a consequent modification of the semiconductor properties. Cross section measurements of neutron induced reactions on GaAs are thus important for the characterization of the semiconductor and how it might be affected by the neutron and high radiation environments. Such studies are of interest to the applications concerning national security and the stockpile stewardship program.

In general, such cross section measurements are equally important for basic research. The experimental results can help test the different statistical model codes and contribute to constraining the parameter set used therein. Such studies are also expected to provide significant

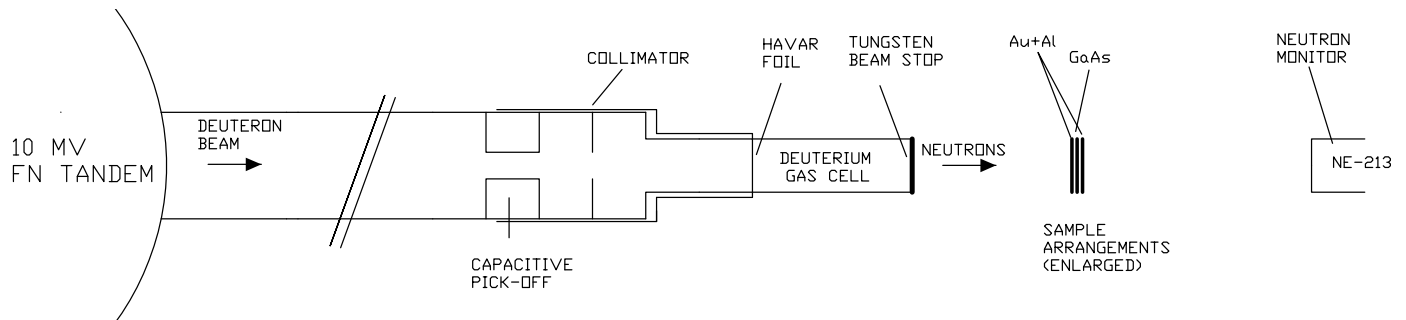


Figure 1. Schematic representation of the experimental setup at the Neutron Time-of-Flight Area of the 10 MV FN Tandem in Triangle Universities Nuclear Laboratory.

insight into the reaction mechanisms dominant at different energy regimes.

The present work reports the cross section measurements on five reactions $^{69}\text{Ga}(n, 2n)^{68}\text{Ga}$, $^{69}\text{Ga}(n, p)^{69m}\text{Zn}$, $^{71}\text{Ga}(n, p)^{71m}\text{Zn}$, $^{75}\text{As}(n, 2n)^{74}\text{As}$, and $^{75}\text{As}(n, p)^{75}\text{Ge}$, over an energy range from 7.5 to 15 MeV.

2. Experimental Details

Neutron activation of the GaAs foils was carried out at the 10 MV FN Tandem Accelerator in Triangle Universities Nuclear Laboratory (TUNL). The monoenergetic neutron beams were produced via the $^2\text{H}(d, n)^3\text{He}$ reaction. The deuterium gas was filled into a 3 cm long cylindrical cell, at pressure of around 2 atm, and sealed from the beamline vacuum by a 0.635 mm thin Havar foil. The pressure in the gas cell and the energy losses of the deuteron beam in the Havar foil contributed to the energy spread of the neutron beam.

The GaAs samples, 99.9% pure and cut into dimensions $1\text{ cm} \times 1\text{ cm}$, were mounted normal to the incident beam, at a distance of 2.6 cm downstream from the exit window of the gas cell. Natural Al and Au foils, also cut into $1\text{ cm} \times 1\text{ cm}$ dimensions, were mounted on either face of the GaAs samples and irradiated together, for estimating the neutron neutron flux incident on the samples. The schematic representation of the experimental arrangement is illustrated in Figure 1. The large (more than 10 m) open space around the gas cell in the experimental area minimized the "room-return" neutrons.

The GaAs foils were irradiated at ten different neutrons energies, $E_n(\Delta E_n) = 7.5(2), 8.0(1), 8.5(2), 9.5(1), 10.2(1), 11.0(1), 11.5(1), 12.5(1), 13.25(10), 14.0(1), 14.5(1)$ and $15.0(1)$ MeV. The neutron flux, during each irradiation, was monitored using a NE-213 liquid scintillator detector and was kept constant throughout the activation run. The beam current and the neutron flux incident on the samples was $\sim 10^7\text{ s}^{-1}$. At each neutron energy, two separate irradiation runs were carried out, one being for a shorter (around 3 hours) duration while the other for a long (around 15 hours) period. without causing any saturation in their decay. However at the highest energies 14, 14.5 and 15 MeV, only a single run, of around 6 hours, was carried out.

Following the irradiations, the samples were measured, using HPGe detectors, in the TUNL

Table 1. Neutron induced reactions on GaAs and monitor foils measured in the present work.

Reaction Channel	Product Half-life	Q-value (keV)	E_γ (keV)	I_γ (%)
GaAs Reactions				
$^{69}\text{Ga}(n, 2n)^{68}\text{Ga}$	67.71 m	-10312.95	1077.34	3.22
$^{69}\text{Ga}(n, p)^{69m}\text{Zn}$	13.76 h	-127.44	438.634	94.77
$^{71}\text{Ga}(n, p)^{71m}\text{Zn}$	3.96 h	-2031.0	386.28	93
$^{75}\text{As}(n, 2n)^{74}\text{As}$	17.77 d	-10243.76	634.78	15.4
$^{75}\text{As}(n, p)^{75}\text{Ge}$	82.78 m	-393.63	264.6	11.4
Monitor Reactions				
$^{197}\text{Au}(n, 2n)^{196}\text{Au}$	6.1669 d	-8072.39	355.73	0.87
$^{27}\text{Al}(n, \alpha)^{24}\text{Na}$	14.997 h	-3132.14	1368.626	99.9936

low background counting facility. One 60% HPGe detector was used to count the GaAs samples while the Au and Al monitor samples were measured in a 20% extended range HPGe detector. The detectors were elaborately shielded against room and cosmic background radiations. The samples being measured were placed in aluminium containers and positioned at a fixed distance of 3 cm from the respective detector. The efficiency and the energy calibrations of the HPGe detectors were carried out with the standard radioactive sources ^{152}Eu , ^{60}Co , ^{133}Ba and ^{137}Cs . The data acquisition system used in the offline measurements was Canberra Multiport II MCA, supported by the GENIE 2000 software.

3. Data Analysis

The acquired gamma-ray spectra, from the offline measurements of the activated samples, were analyzed to identify the reaction products and estimating the respective peak areas using the software Tv [1]. In the present work only the products with half-lives of ~ 1 hour or more have been studied. Table 1 lists the different reaction channels studied in the present measurements along with the half-lives of the products and the gamma-ray transition energies used to identify and calculate the respective cross sections. In addition, Table 1 lists the reactions on the Au and the Al monitor foils, used for the flux normalization. The half-lives of the products of interest were also estimated from the cycle measurements of the activated samples and compared with the adopted values. They are in good agreement with the established values, as recorded in Table 1 from the National Nuclear Data Center database Nudat 2.5. The branching ratios for the gamma transitions and the Q-values for the reaction channels of interest are also quoted.

The cross section for the reaction channels of interest was calculated from the well known activation formula according to which the induced activity is given by,

$$A = \sigma \phi n (1 - e^{-\lambda t_i}) e^{-\lambda t_d} (1 - e^{-\lambda t_m}) \quad (1)$$

Table 2. Sources and approximate magnitudes (in %) of the uncertainties in the present cross section measurements.

Uncertainty	Magnitude (%)
Statistics	1-2
Sample mass	< 1
Detector efficiency	2-3
Branching ratio	≤ 1
Product half-life	≤ 1
Monitor cross section	1-4 ($^{27}\text{Al}(n, \alpha)$) 1-4 ($^{197}\text{Au}(n, 2n)$)
Low energy neutrons	< 1
Total	3-5

σ being the cross section, ϕ is the incident flux, n is the number of target nuclei, t_i is the irradiation time, t_d is the decay time before the commencement of the offline counting and t_m is the measurement time. The induced activity is represented by the peak area of the respective gamma transition normalized by the corresponding branching ratio, the disintegration rate of the radioactive product and the absolute efficiency of the detector.

The cross section was corrected for the contribution from the low energy neutrons using,

$$C_{bu} = 1 - \frac{\int_0^{E_{max}^{bu}} \sigma(E)Y(E)dE}{\int_0^{E_{max}} \sigma(E)Y(E)dE} \quad (2)$$

where $Y(E)$ is the relative yield of the neutrons with energy E and $\sigma(E)$ is the cross section of the reaction under consideration. E_{max}^{bu} is the maximum energy of the break-up neutrons and the E_{max} is the maximum energy of the neutron beam, including the energy spread. The integrals were solved numerically by interpolating the neutron spectrum and the excitation function to the same energy grid. The correction required due to interference from the low energy neutrons depends on the specific reaction, the respective threshold and the shape of the excitation function. Since the present measurements were carried out in the same experimental conditions as in [2], the same analysis has been applied to the break-up corrections described in Eq. (2).

The sources and the magnitudes of the average uncertainties in the present measurements are summarised in Table 2. It is noteworthy that the statistical uncertainty was as high as 7% near threshold energies and for specific reactions the total uncertainty was 10-11%. Also, the uncertainty on the $^{197}\text{Au}(n, 2n)$ monitor reaction cross-section is 8-12% below 12 MeV incident neutron energy [3].

4. Results and Discussions

The cross section measurements on Ga and As isotopes in the energy range from $E_n = 7.5$ to 15 MeV is shown in Figure 2 along with the results from the statistical model calculations, the latest evaluations, and the literature data. The statistical model calculations were carried out

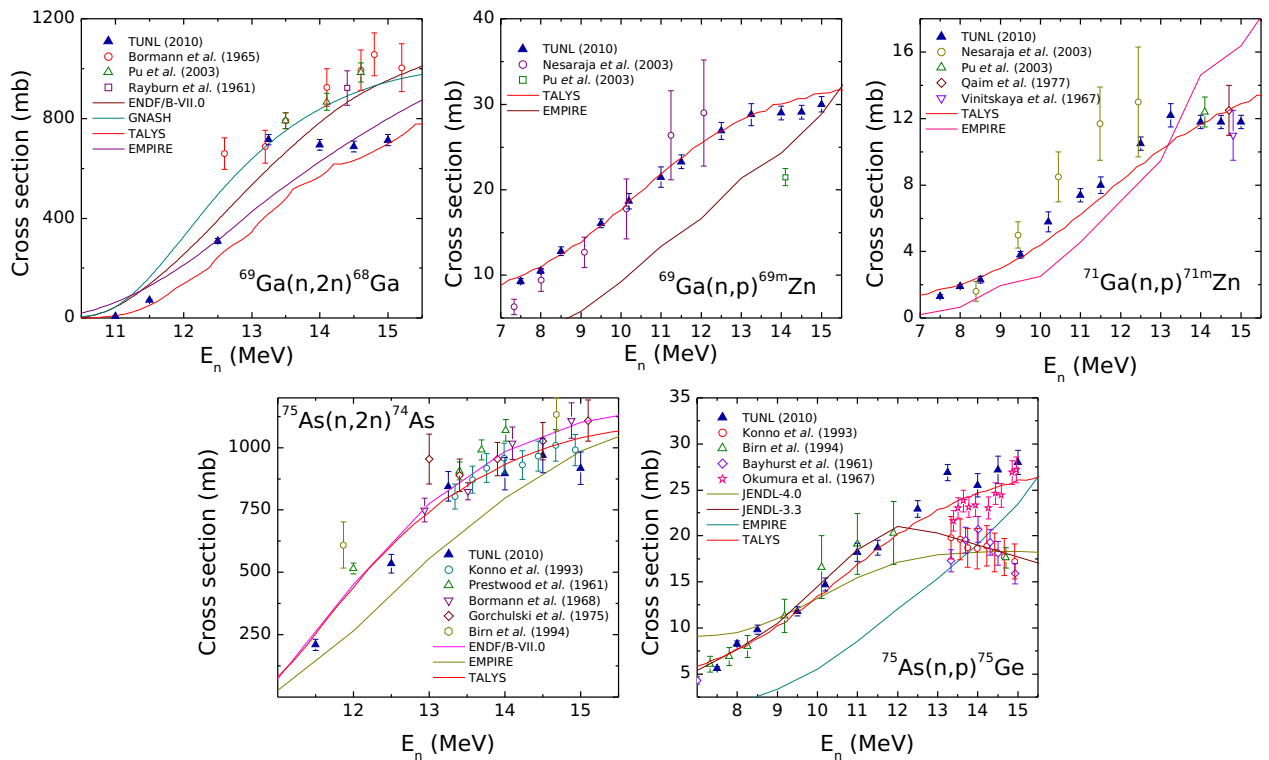


Figure 2. Plots of the present cross section measurements as a function of the neutron energy for the reactions under study.

using the codes TALYS [4] and EMPIRE [5].

The cross section results for the $^{69}\text{Ga}(n,2n)^{68}\text{Ga}$ reaction, from the present work, are consistently lower than the previously reported values for the same. In view of this discrepancy, the measurements at higher energies were repeated to confirm the quoted cross-section results. For the $^{69}\text{Ga}(n,p)^{69m}\text{Zn}$ reaction, the measured cross sections in the present work are in good agreement with the results of Nesaraja *et al.* [6], within the uncertainty quoted by the latter. The results from Pu *et al.* [7] at a single energy $E_n = 14$ MeV is discrepant with respect to the shape of the excitation function set by the present measurements. As far as the $^{71}\text{Ga}(n,p)^{71m}\text{Zn}$ reaction is concerned, the cross section values from the present measurements agree with Nesaraja *et al.* [6] at lower energies. At higher energies, the results of Nesaraja *et al.* [6] are larger than the present work, and with substantial uncertainties. The present measurements also agree well with the measurements of Pu *et al.* [7] and Qaim *et al.* [8] around 14 MeV while that of Vinitkaya *et al.* [9] is somewhat low, though overlapping with the present measurements, within the quoted uncertainty.

The measured cross section of the $^{75}\text{As}(n,2n)^{74}\text{As}$ reaction from the present work is lower

than the available literature data at lower neutron energies. At energies above 13 MeV the present measurements agree well with that of Konno *et al.* [10, 11] but that by Prestwood *et al.* [12], Grochulski *et al.* [13], and Birn *et al.* [14] are consistently higher over the entire energy range. Interesting observations are made for the $^{75}\text{As}(n,p)^{75}\text{Ge}$ reaction with respect to the literature data. The present measurements show a continuously increasing cross section for this reaction in the energy range of 7.5 to 15 MeV, as illustrated in Figure 2. The measured cross section agrees well with the data from Birn *et al.* [14] below 13 MeV. However, above 13 MeV, nearly all the existing literature data, from Birn *et al.* [14], Konno *et al.* [10, 11] and Bayhurst *et al.* [15], shows a decrease in the cross section while the present measurement shows a continuous increase. In this respect, the measurements by Okumura *et al.* [16] are closer to the present results, with increasing cross sections at higher energies.

5. Summary and Conclusions

Cross section measurements were carried out for neutron induced reactions on Ga and As isotopes in the energy range from 7.5 to 15 MeV. Monoenergetic neutron beams, pure samples and high resolution HPGe detectors were used to restrict the uncertainties in the measurements. The cross section results were compared with the literature data and found largely to be in satisfactory compliance. Statistical model calculations were carried out based on the Hauser-Feshbach formalism using different codes and are in good agreement with the present measurements. This work has contributed to the understanding of the neutron induced reactions on the individual Ga and As isotopes, that can be extrapolated to the behavioural interpretations of the GaAs semiconductor in the high radiation environments. The said understanding can be applied to the issues pertaining to the national security viz., nuclear forensics and the stockpile stewardship program.

This work is supported in part by the National Nuclear Security Administration (NNSA) under the Stewardship Science Academic Alliance Program through the US Department of Energy grant DE-PS52-08NA28920, DE-FG52-06NA26155 and by Los Alamos National Laboratory (W-7405-ENG-36).

References

- [1] Theurkauf J, Esser S, Krink S, Luig M, Nicolay N, Stuch O, Wolters H *Tv Program*
- [2] Tonchev A P, Angell C T, Boswell M, Crowell A S *et al.* 2008 *Phys. Rev. C* **77** 054610
- [3] José Martínez-Rico 1993 *INDC(NDS)-285 Distr. G*
- [4] Koning A J, Hilaire S and Duejvestijin M C 2008 *Proc. Int. Conf. on Nuclear Data for Science and Technology* (Nice) p 211
- [5] Herman M, Capote R, Carlson B V, Obložinský P, Sin M, Trkov A, Wienke H, Zerkin V 2007 *Nucl. Data Sheets* **108** 2655
- [6] Nesaraja C D, Sudar S and Qaim S M 2003 *Phys. Rev. C* **68** 024603
- [7] Pu Z, Yang J and Kong X 2003 *App. Rad. Iso.* **58** 723
- [8] Molla N I and Qaim S M 1977 *Nucl. Phy. A* **283** 269
- [9] Vinitskaya G P, Levkovskiy V N, Sokol'sky V V and Kazachevskiy I V 1967 *Yad. Fiz.* **5** 1175
- [10] Konno C, Ikeda Y, Oishi K, Kawade K, Yamamoto H and Maekawa H 1988 *JAERI Report* **1312**
- [11] Konno C, Ikeda Y, Oishi K, Kawade K, Yamamoto H and Maekawa H 1993 *JAERI Report* **1329**
- [12] Prestwood R J and Bayhurst B P 1961 *Phys. Rev.* **121** 1438
- [13] Grochulski W, El-Konsol S and Marcinkowski A 1975 *Act. Phys. Pol. B* **6** 139
- [14] Birn I and Qaim S M 1994 *Nucl. Sci. Eng.* **116** 125
- [15] Bayhurst B P and Prestwood R J 1961 *Jour. Inorg. Nucl. Chem.* **23** **173**
- [16] Okumura Shoji 1967 *Nucl. Phy. A* **93** 74